Journal of Energetic Materials
Publication details, including instructions for authors and subscription information:
http://www.informaworld.com/smpp/title~content=t713770432

Mechanical Properties of Confined Explosives

Donald A. Wiegand[a]; Brett Reddingius[a]
[a] U.S. Army Armament Research, Development and Engineering Center, Picatinny Arsenal, NJ, USA

To cite this Article Wiegand, Donald A. and Reddingius, Brett(2005) 'Mechanical Properties of Confined Explosives', Journal of Energetic Materials, 23: 2, 75 — 98
To link to this Article: DOI: 10.1080/07370650590936415
URL: http://dx.doi.org/10.1080/07370650590936415

Energetic Materials, 23: 75–98, 2005

ISSN: 0737-0652 print
DOI: 10.1080/07370650590936415

Taylor & Francis
Taylor & Francis Group

Mechanical Properties of Confined Explosives

DONALD A. WIEGAND
BRETT REDDINGIUS

U.S. Army Armament Research, Development and Engineering Center, Picatinny Arsenal, NJ, USA

The mechanical properties of composite explosives are being studied as a function of mechanical confinement. Although other techniques for confinement were used, most of the results presented here were obtained by the use of a constant confining pressure obtained by oil immersion. While many energetic materials fail by crack processes when unconfined, with all of the forms of confinement used here they appear to fail by plastic flow. For crystalline explosives, for example, TNT and composition B, the yield strength and the modulus are independent of confining pressure. However, for materials containing polymer binders such as plastic-bonded explosives, these properties are found to significantly increase with pressure.

Keywords: confinement, pressure, flow stress, modulus, work hardening, work softening, plastic bonded explosive, crack, fracture, plastic deformation, mechanical properties

Introduction

Energetic materials are often used under conditions of mechanical confinement, for example, explosives by the steel casings

Address correspondence to Donald A. Wiegand, U.S. Army Armament Research, Development and Engineering Center, Bldg 3022, Picatinny Arsenal, NY 07806, USA. E-mail: dwiegland@pica.army.mil

and propellants by the breach and the high pressures during burning. When modeling the response of energetic materials to planned and unplanned mechanical stimuli, it is necessary to know the mechanical failure modes and other mechanical properties as a function of confinement. Previously reported studies indicate a change with confinement in failure modes but not elastic properties for compression of polycrystalline explosives, that is, TNT (trinitrotoluene) and Composition B, a composite of TNT and RDX (cyclotrimethylene trinitramine) [1,2]. In addition, the yield strength observed with confinement is independent of confining pressure [2]. The sample loading conditions for this work is shown in Figure 1, and some results for Composition B are given in Figure 2. While studies of

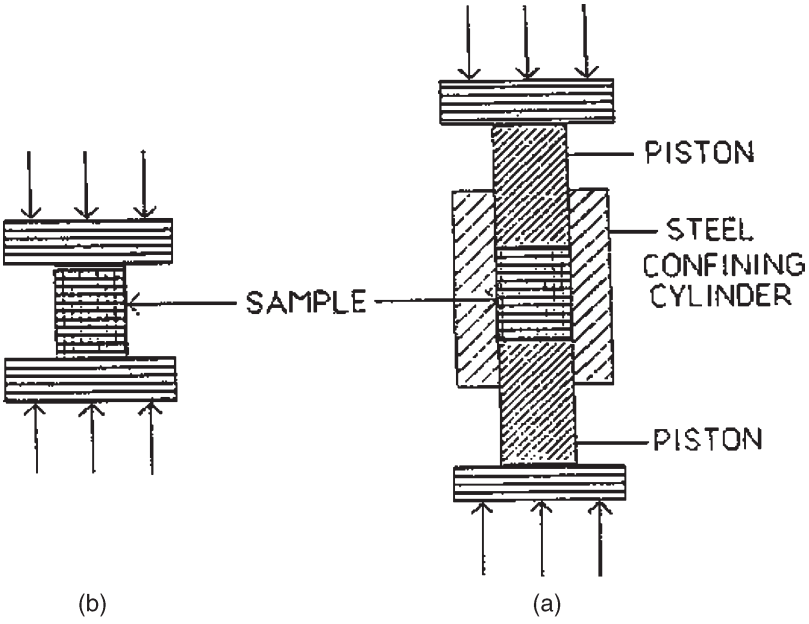

Figure 1. Sample and platen arrangements for (a) unconfined compression and (b) confined compression in a thick-walled steel cylinder. The samples are cylindrical and are compressed along the cylinder axis in each case.

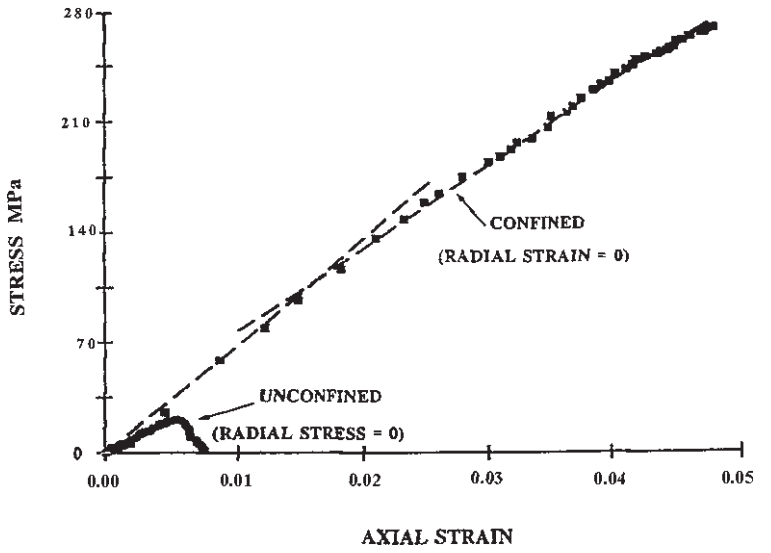

Figure 2. Axial stress versus axial strain for Composition B for the conditions of Figure 1.

composite plastic-bonded explosives also indicate a change in compressive failure mode with confinement, use of the same steel cylinder technique as used for TNT and Composition B indicates that the results cannot be interpreted in terms of properties independent of confining pressure [3]. The work reported here was undertaken to investigate the confining pressure dependence of failure and other mechanical properties of plastic-bonded explosives.

Experimental

A high-pressure chamber designed to contain pressures up to 138 MPa was used to study the compressive mechanical properties as a function of confining pressure [4,5]. Hydraulic oil was used as the confining medium, and the sample in the form of a right circular cylinder was protected from the oil by a tight-fitting tubular gum rubber or neoprene shroud. A sketch of the sample, shroud, and sensors is given in Figure 3. The ends

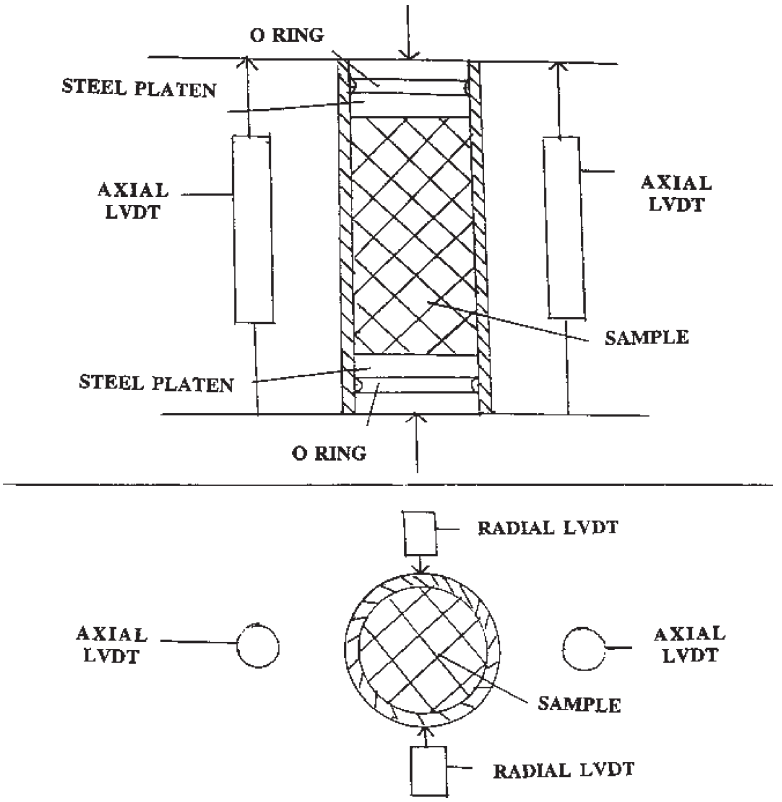

Figure 3. Side and end sketches of the sample, shroud, and sensors for compression at constant pressure.

of the sample were against steel platens, and O-ring seals were used to prevent oil from reaching the sample. The samples were compressed along the cylindrical axis, and two LVDTs (linear voltage differential transformers) were mounted to measure axial strains. They were spaced 180° apart around the circumference of the sample with their axes parallel to the sample axis. The sample axial strain was taken as the average of the strains obtained from the two LVDTs. Two or in some cases three additional LVDTs were mounted to measure radial strains. They were placed in a plane at the sample axial midposition with their axes perpendicular to the sample axis. They

were also 180° (or 120° for three radial LVDTs) apart around the sample circumference. The confining pressure is taken here as the cell hydrostatic pressure before the start of and/or during the the axial compression. Measurements at atmospheric pressure were made in air.

Axial stress versus axial strain data in compression were obtained using the above chamber and an MTS servo-hydraulic system operated at a constant displacement rate [1,6]. Most of the work was carried out at a strain rate of approximately 0.001/sec, but some samples of EDC37 [7] were compressed at a rate of approximately 0.0005/sec. In addition, one sample of each PBS 9501, PAX2A, and EDC37 were compressed at strain rates two orders of magnitude higher than the above strain rates, and LX-14 samples were compressed over a range of strain rates. The right circular cylinder samples were 3.81 cm (1.50 inch) in length and 1.90 cm (0.75 inch) in diameter and so had a length-to-sdiameter ratio of two. The end faces of all samples were coated with a lubricant to minimize frictional effects between the sample end faces and the loading platens. The sample temperatures during measurements were between 20 and 23°C. Samples were conditioned at temperature for at least 2 hr before measurement. The dimensions of all samples at 0.1 MPa (atmospheric pressure) were used to obtain engineering stress and engineering strain.

Most of the results presented here of measurements in the high-pressure chamber are for a composite, PBS 9501, containing 94% sucrose, an inert, and a binder (see Table 1). This composite was developed as an inert mechanical mock for a plastic-bonded explosive, PBX 9501, composed of 95% HMX and the same binder [13]. The unconfined compressive mechanical properties of PBS 9501 are similar to those of PBX 9501 [13]. Some results of measurements in the high-pressure chamber are also presented and/or discussed for PBX 9501 and three other composite plastic-bonded explosives, LX-14, PAX 2A, and EDC37 [7] (see Table 1). Results for other types of confinement are presented and/or discussed for Compositions B, PBX 9501, PBX 9404, PBX 9502, and PAX 2A. Some of these explosive formulations were compressed at atmospheric pressure as a

Table 1
Composition of explosive composites considered in this study

Name	Explosive/Inert	Binder		T_g (°C)
		Polymer	Plastizer	
PAX2A	HMX	CAB	BDNPA/F	−37 [8]
	85%	6%	9%	
PBS 9501	Sucrose	Estane	BDNPA/F	−41(B) [9]
	94%	3%	3%	
PBX 9404	HMX	NC[a]	CEF	−34 [10]
	94%	2%	3.84%	
PBX 9501	HMX	Estane	BDNPA/F	−41(B) [9]
	95%	2.5%	2.5%	
PBX 9502	TATB	KEL F 800		+30(B) [10]
	95%	5%		
LX-14	HMX	Estane		−31(B) [10]
	95.5%	4.5%		
EDC37 [11]	HMX	NC	DNEB/TNEB	−63(B) [12]
	91%	1.0%	5.22%/2.78%	
Composition B	RDX	TNT	WAX	
	59.5%	39.5%	1%	

Nomenclature: HMX: Cyclotetramethylene tetranitramine. TATB: 1,2,5-triamino-2,4,6–trinitrobenzeene. RDX: Cyclotrimethylene trinitramine. NC: Nitrocellulose. CAB: Cellulose acetate butyrate. BDNPA/F: Bis(2,2-dintropropyl)acetal/formal. CEF: Tris(beta chloroethyl) phosphate. Estane: Polyurethane. KEL F 800: Chlorotrifluoroethlene/vinylidine fluoride copolymer. DNEB: Dinitroethylbenzene. TNEB: Trinitroethylbenzene. B: Property of the binder.

[a] Also contains 2% etrhyl centralite.

function of sample length-to-diameter ratio. Samples of the composites were prepared by pressing or casting (Composition B) into large billets and machining to size. Precautions were taken to ensure that the cylinder end faces were adequately flat and parallel [13–15]. The densities of all samples were in a narrow range close to the maximum theoretical (zero porosity) density. All sensors were calibrated by the manufacturer or calibrated against standards provided by the manufacturer. It is estimated that variations from sample to sample in any measured quantity are significantly greater than errors introduced by the sensors or errors introduced during data processing.

Results

In Figure 4 the compressive axial stress-strain response of PBS 9501 is given for several confining pressures [16,17]. There are significant differences between the curves for the lower confining pressures and the curves for the higher confining pressures. These include (a) a maximum stress for the lower confining pressures that is not observed at the higher confining pressures, and (b) a change from strain softening after the maximum at

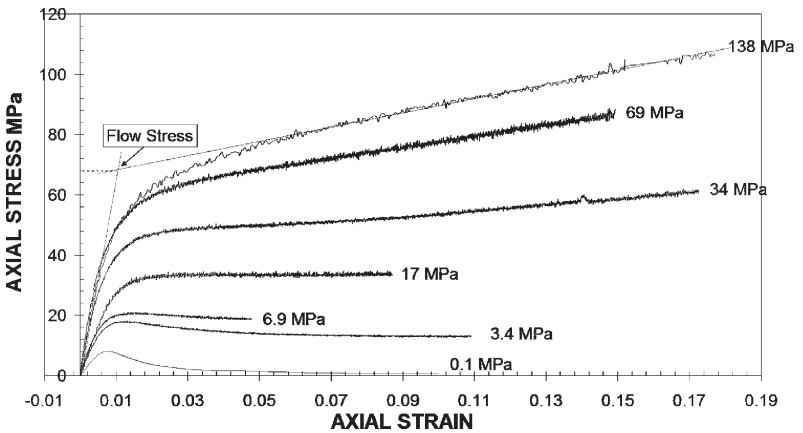

Figure 4. Axial stress versus axial strain for samples of PBS 9501 for confining pressures from bottom to top of 0.1 (atmospheric), 3.4, 6.9, 17, 34, 69, and 138 MPa.

the lower confining pressures to work hardening at larger strains at the higher confining pressures. In addition, the initial slope is larger at the higher confining pressures. Young's modulus is defined as the initial slope at atmospheric pressure. This initial slope at higher confining pressures is referred to here simply as the modulus.

A yield strength, taken at the point at which the initial part of the stress-strain curve deviates from linearity (Figure 4), has been found to be variable from sample to sample and is not considered here. A yield strength obtained by a strain offset technique has much less variation from sample to sample and is used in some cases. However, in most cases a flow stress is used to characterize the data. This flow stress is taken as the stress at the intersection of a straight line fitted to the work-hardening part of the stress-strain curve with the straight line fitted to the initial modulus portion of the curve. This is indicated in Figure 4 for the data at 138 MPa and is the stress at which significant plastic flow occurs. For PBS 9501 this flow stress is numerically very close to the yield strength as obtained by a 1% strain offset method. The flow stress at the lower pressures is taken as the maximum stress.

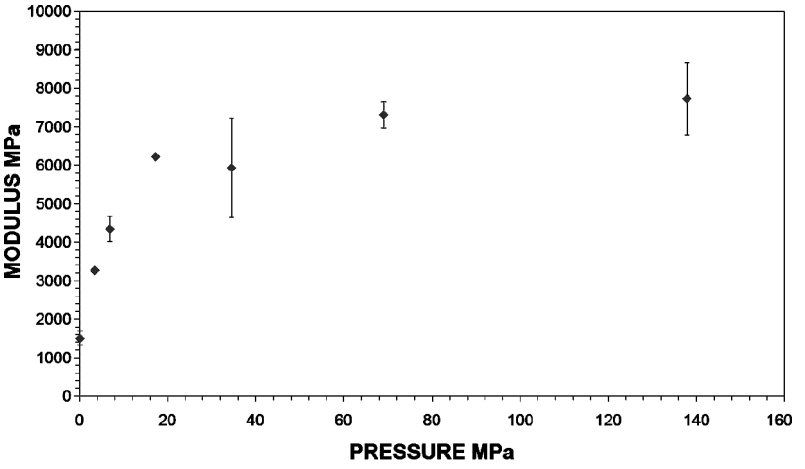

Figure 5. Modulus versus confining pressure for PBS 9501.

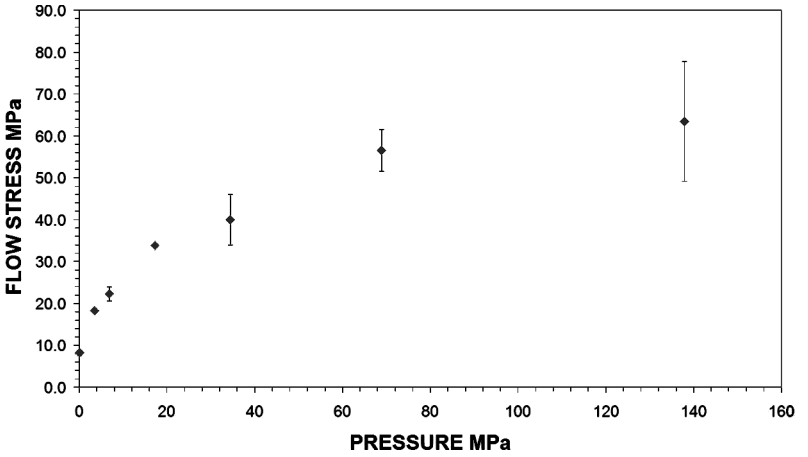

Figure 6. Flow stress versus confining pressure for PBS 9501.

As shown in Figure 5, measurements as a function of confining pressure indicate that the modulus increases at a continually decreasing rate as pressure is increased. Thus, the initial rate of change of the modulus with pressure at the lowest pressures is more than an order of magnitude greater than the rate at the highest pressures. A similar rate of increase with pressure is found for the flow stress as shown in Figure 6. However, there is too much scatter in the present data to determine if there is a simple relationship between the modulus and the flow stress as a function of pressure. The maximum slope of the stress-strain curve in the work-softening/work-hardening region increases from negative to positive values with increasing pressure, and the rate of increase with increasing pressure also decreases.[1] This is shown in Figure 7. Thus, the whole stress-strain curve becomes less sensitive to pressure at the higher pressures of Figure 4. There is considerable spread in the work-hardening slope at 138 MPa, as indicated by the large error bars of Figure 7 at this pressure. The error bars of Figures

[1]The slope in the work-hardening/work-softening part of the stress-strain curve has also been referred to as the failure modulus [18] and the damage modulus [19].

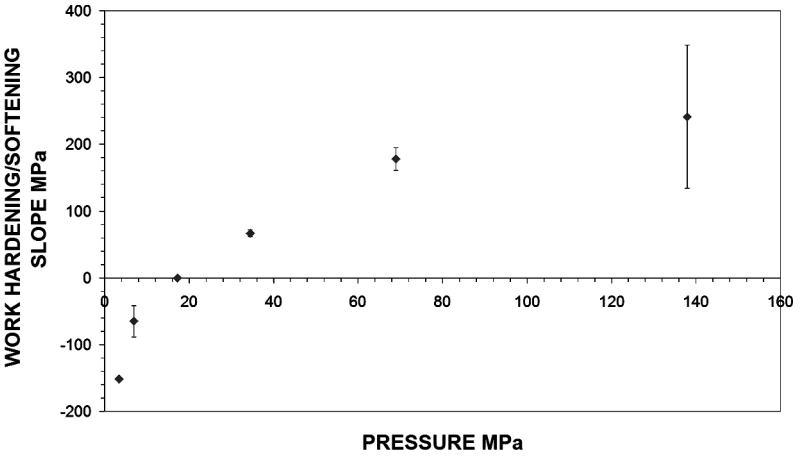

Figure 7. Work-hardening/Work Softening slope versus confining pressure for PBS 9501.

5, 6, and 7 are the standard deviations of the measured values. In these figures each point is the average of the results for two or three samples with the exception of the points at 3.4 and 17 MPa, which represent the results of only one sample in both cases. Increases in the yield strength and the modulus with increasing pressure have been reported for polymers and polymer composites, including gun propellants [20–23].

Results similar to those of Figures 4, 5, 6, and 7 were also obtained for LX-14. In addition, the very limited results for PBX 9501 at the higher pressures of Figure 4 indicate similar shaped stress-strain curves and suggest that the flow stress and the modulus of PBS 9501 may be about 50% larger than the values for PBX 9501 in this pressure range. Additional measurements of PBX 9501 are necessary to confirm these results. Results similar to those of Figure 4 were also obtained for PAX2A and EDC37 [7]. While detailed results for these four composites will be published separately, the stress-strain curves for unconfined and confined PAX2A are given in Figure 8 [24]. For PAX 2A and also for EDC37 at elevated pressures, the stress-strain response has continuous curvature (see Figure 8) so that linear regions are not clearly identifiable. Therefore,

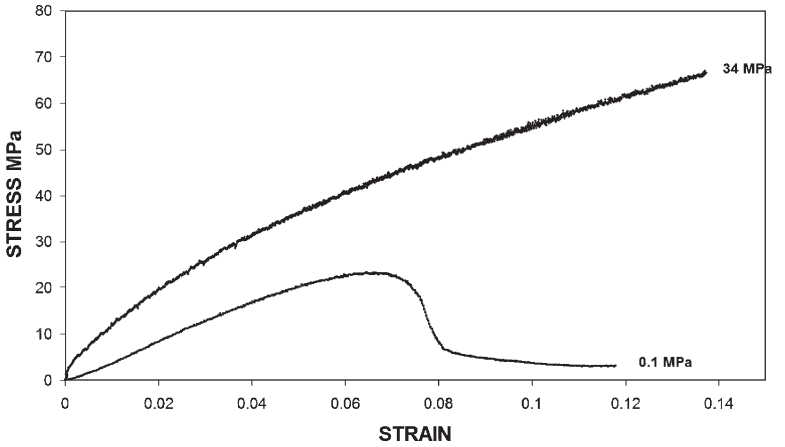

Figure 8. Axial stress versus axial strain for PAX 2A with confining pressures from bottom to top of 0.1 MPa (atmospheric) and 34 MPa.

the strain offset method is used to obtain a measure of the yield strength, and the modulus is taken as the initial slope of the stress-strain curves. The work-hardening coefficient is taken as the average slope at larger strains.

As shown in Figure 2, the results for samples compressed axially while radically confined in a thick-walled steel cylinder are similar in part to the confined case of Figures 4 and 8 [2]. However, for large strains of the curve of Figure 2 the slope is determined primarily by the bulk modulus. This is not the case for the confined curves of Figures 4 and 8.

The strain softening at 0.1 MPa (lowest curves of Figures 2, 4, 8, and 10; see below) has been attributed to damage due to crack growth processes [24,25]. Therefore, the results of these figures suggest that this crack growth does not occur at the higher pressures where work softening is not observed. Thus, there appears to be a shift from work softening due to crack growth at low confining pressures to work hardening and plastic flow at higher pressures. The photograph in Figure 9 shows pictorial evidence to support this postulate of a change in failure processes with increasing pressure. The sample compressed at

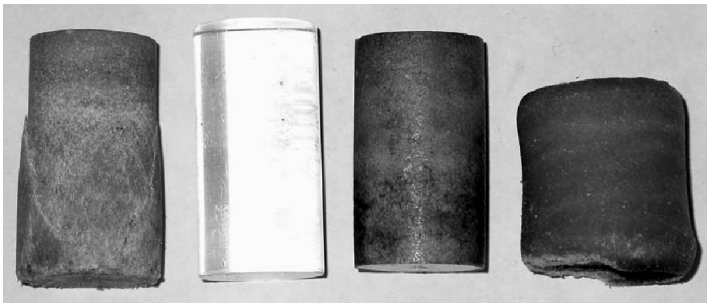

Figure 9. Photograph of deformed samples of PBS 9501 and a reference plastic sample of the same dimensions as the PBS 9501 samples before deformation. From left to right: sample compressed axially with a confining pressure of 0.1 MPa; plastic reference sample; samples compressed axially with confining pressures of 138 MPa, and 69 MPa. The maximum axial strain differs for each sample. The sample deformed at 138 MPa was graphite coated before deformation.

0.1 MPa shows extensive surface cracking while the samples compressed at 69 and 138 MPa show no evidence of surface cracking. The total axial strain was different for each sample of Figure 9, and it is clear from the figure that the retained or permanent axial strains also differ for each sample. The sample compressed at 0.1 MPa has, in addition to extensive cracking, a large radial expansion at the bottom but negligible radial expansion at the top. A gradient of radial strain is often observed for this type of sample, this amount of axial compression, and this confining pressure (atmospheric). The permanent axial strain for this sample is -5.2%. Gradients of radial strain (barreling) were also observed at the lower confining pressures (not shown), for instance, at and below 34 MPa, but surface cracking was not observed with confinement.

For samples compressed at 34 MPa (not shown in Figure 9) and at higher pressures, the radial strain is much more uniform along the sample length than for samples compressed at lower pressures. The permanent axial and radial strains are -9.3% and 4.7% for the sample compressed at 138 MPa and

−38.8% and 27.1% for the sample compressed at 69 MPa (Figure 9). The permanent radial strains are actually somewhat larger at the ends than along the rest of the sample for these samples. This apparently occurs because of plastic flow of the sample along the sides of the steel compression platens. Before compression the sample and platen diameters are equal. However, with axial compression the sample diameter increases much more than the diameter of the steel platens. Therefore, regions of the sample near the circumference at each end of the sample are not in contact with the respective platen, and so plastic flow along the cylindrical side surfaces of the platens takes place. Because of this effect, the sample ends are recessed, and the permanent axial strains given above were measured in the recessions. The permanent radial strains were measured in regions of uniform radial strain away from the sample ends.

The densities of most samples (with the exception of PBS 9501) were measured before and after compression by weighing in air and in purified water. The density of the water was taken at the measurement temperature. The density changes (density before compression minus density after compression, both at atmospheric pressure) of the samples that were compressed while confined hydrostatically (see Figure 3 and associated discussion) are small and less than 0.5% in most cases for permanent axial and radial strains of approximately −15% and 8%, respectively, and for confining pressures of 34 MPa or greater. Both positive and negative density changes were observed. For LX-14 at confining pressures of 34 MPa or greater, the absolute value of the ratio of the fractional density change to the permanent axial strain is about 0.028. At lower confining pressures some barreling of samples was observed, and the density changes are somewhat larger. For larger permanent strains larger density changes are also generally observed. The density change of only one sample of PBS 9501 was determined because of the difficulty of obtaining the weight in water, which in turn is due to the solubility of sucrose in water. Since the density changes for all samples are small compared to the permanent axial and radial strains, it is suggested that the samples have

deformed primarily at constant volume and without extensive internal open crack generation.

The results given in Figures 5, 6, and 7 indicate that the modulus, the flow stress, and the work-hardening coefficient increase with increasing pressure. In addition, at 138 MPa and at the strain rates of interest for military applications (see below) the estimated yield strengths of PBS 9501, LX-14, PBX 9501, PAX2A, and EDC37 are less than but approach a nominal value for aluminum of 100 MPa (at 0.1 MPa) and are small but nontrivial fractions of a nominal value for annealed steel of 275 MPa (also at 0.1 MPa) [26,27]. Therefore, at the higher confining pressures used in this work these five composites have some metal-like properties, that is, they fail by plastic flow, exhibit work hardening, and the yield strengths of all five at the highest pressures and high strain rates approach the values of metals. This behavior is to be contrasted with the sometimes brittle ceramic-like properties when these types of materials are unconfined (see Figures 2, 4, 8, and 10; see below).

All of the results presented above were obtained using a strain rate of either 0.0005/sec (EDC37) [7] or 0.001/sec. Results for LX-14 at 69 MPa as a function of strain rate indicate that the flow stress increases linearly with the log of the strain rate [24]. The responses of PBS 9501, PAX2A, and EDC37 under confined conditions indicates that the flow stress of all three composites also increased with an increase in strain rate of two orders of magnitude. The effect of strain rate on the modulus is inconclusive at this time, and the work-hardening slope showed no consistent trend with changes in strain rate for all four materials. Additional studies of the effect of strain rate on the stress-strain response of confined plastic-bonded composites are in progress.

As noted above, measurements were also made of the radial displacement at the sample midplane. However, the radial displacements obtained in this way at elevated pressures are the sum of the displacements for the sample and the shroud. A meaningful separation of the measured displacements to obtain the radial displacements and so the radial strains of the samples has not been made. However, at atmospheric pressure

measurements were made without the shroud. From the slope of the radial strain versus axial strain curve obtained at atmospheric pressure the value of Poisson's ratio is found to be about 0.37 for PBS 9501 and very close to 0.5 for PAX2A.

Results qualitatively similar to those of Figures 4 and 8 have been obtained for several composites including PBX 9404, PBX 9501, PBX 9502, PAX2A, and Composition B by varying the sample length (L) to diameter (D) ratio, L/D [15,24]. Uniaxial stress-strain curves in compression for cylindrical samples with L/D ratios from 0.08 to 1.0 are given in Figure 10 for PBX 9501. The curve for the smallest value of L/D is similar to the data of Figures 4 and 8 for the higher confining pressures, while the curves for the larger values of L/D are similar to the data at the lower pressures of Figures 4 and 8. Thus, the effect on the stress-strain curve of decreasing L/D in Figure 10 is very similar to the effect of increasing the confining pressure as shown in Figure 4, and the transition from strain softening to work hardening is also a function of L/D. Therefore, it appears that crack growth processes and the resultant strain softening are reduced and that there is a shift in the primary deformation mechanism from crack processes to plastic flow as L/D is decreased [15]. An examination of the samples after deformation indicates that the samples having the smallest value of L/D contain cracks and some fractures in regions at the periphery of the samples. These regions have dimensions in the radial direction comparable to the sample lengths. The remaining inner portions of these samples are not fractured, do not have visible cracks, appear to be plastically deformed, and have permanent axial strains of about -20%. Thus, for this geometry there is apparently a spacial separation of the samples into regions of primarily crack damage and regions of primarily plastic deformation, and so a spacial separation into regions undergoing primarily work softening and regions undergoing primarily work hardening. For the smallest value of L/D the inner regions of the samples away from the periphery are apparently effectively confined by the sample geometry and the platens so that cracking takes place predominantly near the free surfaces at the periphery where

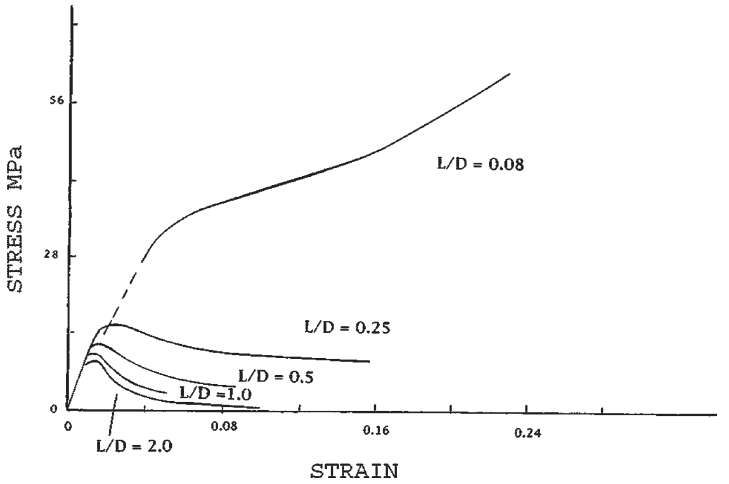

Figure 10. Axial stress versus axial strain for PBX 9501 for cylindrical samples with length/diameter (L/D) ratios of 2.0, 1.0, 0.5, 0.25, and 0.08.

confinement is less. For the larger values of L/D of Figure 10 a separation of the samples into regions of primarily crack damage and regions of primarily plastic deformation damage is not as clear. Small angle neutron and X-ray scattering of the samples having the smallest value of L/D indicate a significant increase in the explosive-binder surface area [28]. This increase in explosive-binder surface area is interpreted as indicating fracture of explosive particles and the flow of binder to cover the new surfaces. Increases in pore surface areas were also observed. Similar damage may then exist in the samples of Figure 4.

A flow stress can be obtained from the upper curve of Figure 10 in much the same manner as it was obtained from the upper curves of Figure 4. From measurements of thin wafers of PAX 2A as a function of temperature and strain rate, a qualitative measure of the flow stress as a function of these parameters has been obtained [24]. This flow stress for PAX 2A was found to increase with increasing strain rate and decreasing temperature [24]. The initial slope of the upper

curve of Figure 10 ($L/D = 0.08$) is not meaningful because of instrumental effects.

Discussion

General considerations for a discussion of the pressure dependence of the stress-strain curves of composites include the following: (a) the pressure dependence of the mechanical properties of the individual components of the composites, (b) the effect of pressure on the interfaces of the composite, and (c) the effect of pressure on defects such as voids and cracks [20]. For the composites under consideration, the mechanical properties of interest here for the polymer component are expected to be a function of pressure, while the same mechanical properties for the crystalline components, that is, sucrose or HMX, are expected to be insensitive or independent of pressure [20]. A discussion of the pressure dependence of the modulus and the flow stress is followed by a very brief general discussion of the pressure dependence of the stress-strain curves.

Modulus

Several factors influence the pressure dependence of the modulus including the following: (a) finite elastic strains, (b) collapse of voids, (c) changes of the glass transition temperature, and (d) the relative contributions from the binder and the explosive or sucrose. Because polymers are softer than many materials, the strains are larger, and in many cases it is necessary to consider finite elastic strains rather than the more usual infinitesimal elastic strains. When this is done, the modulus is found to increase linearly with pressure for the conditions of this work [20]. The rate of increase is dependent only on Poisson's ratio at atmospheric pressure and is between approximately three and eight. The initial slope of the curve of the modulus versus pressure for PBS9501 is about 400 (see Figure 5 and attendant discussion) so that finite elastic strains can account for only a small part of this initial slope. However, finite elastic strains may account for the slope at the highest pressures of Figure 5.

The collapse of voids and cracks may account for a part of the initial increase of the modulus with increasing pressure. The porosities of the undeformed PBS9501 samples are estimated to be between 2% and 2.4%, and the modulus is exponentially dependent on porosity for some types of porosity [29,30]. However, measurements of a group of PAX 2A samples pressed to a range of densities indicate a change of only about 22% in Young's modulus for a 4.2% change in porosity [24]. In addition, data for a group of Composition B samples indicate a change of Young's modulus of 63% for a change of porosity of 2% [30]. These results suggest that only a part of the modulus increase for PBS9501 with pressure as given in Figure 5 can be associated with a decrease in porosity. It is also to be noted that for the collapse of porosity to account for a significant part of the initial slope (Figure 5), the pores must collapse at relatively low pressures compared to the much higher pressures used in preparation by pressing. Measurements at elevated pressures as a function of porosity would be useful in determining the role of porosity in the pressure dependence of the modulus.

An increase in the glass transition temperatures (T_g) with increasing pressure can also cause very significant increases of the modulus under appropriate circumstances [20,31]. Since the T_g's of most of the composites considered here are below the measurement temperature (see Table 1), increases in T_g will result in increases in the modulus [31]. The results of measurements of the modulus at atmospheric pressure as a function of temperature would be helpful in estimating the magnitudes of increases in the modulus that could be expected due to increases of T_g. Unfortunately this information is not currently available for PBS 9501. Of course, determining the pressure dependence of T_g would be especially valuable in resolving this matter.

As noted above, it is also necessary to consider the relative contributions to the modulus by the binder and by the explosive or sucrose as a function of pressure. The total strain can be considered to result from displacements in the binder and displacements in the explosive or sucrose. The component of

the total displacement due to the explosive or sucrose is expected to be independent of or insensitive to pressure. However, the component of the total displacement due to the polymer in the binder is expected to decrease with increasing pressure since the modulus of polymers has been found to increase with increasing pressure [20]. Thus, the total displacement and so the total strain is expected to decrease with increasing pressure. Hence the modulus of the composite is expected to increase with increasing pressure as observed. The temperature and strain rate dependence of Young's modulus at 0.1 MPa indicates that the polymer in the binder plays a very significant role in determining Young's modulus at this pressure [32]. However, as pressure is increased and the component of the total displacement due to the binder decreases, the component of the total displacement due to the explosive will become more significant. Thus, at higher pressures the modulus is also expected to be less sensitive to pressure as observed. Therefore, the observed increase of the modulus with increasing pressure and, in addition, the observed decrease in sensitivity of the modulus to pressure with increasing pressure may both be due at least in part to a decrease in the component of the total displacement due to the binder as pressure is increased. Measurements as a function of temperature and strain rate at elevated pressures may be useful in determining the importance of these processes in determining the pressure dependence of the modulus.

In summary the increase of the modulus with increasing pressure may be due to several factors, that is, finite elastic strains, the collapse of porosity, an increase of T_g, and a decreasing contribution of the polymer binder to the total displacement. Additional work is clearly indicated to determine the roles of the mechanisms considered in the increase of the modulus with increasing pressure.

Flow Stress

At atmospheric pressure (0.1 MPa) it is clear that crack processes take place during compression (see Figure 9). It is also

probable that some plastic flow occurs because of the shape and condition of the samples after deformation. It is to be noted that crack growth and plastic flow need not take place in the same part of a composite. For example, cracks may be primarily interfacial while plastic flow may take place primarily within one of the components of the composite, for example, the binder. With increasing pressure the results suggest that crack growth is decreased and that plastic flow is increased. In particular, surface cracking that is observed without confinement is not observed when samples are confined (see Figure 9). In addition, the fractional density changes on deformation under confinement are very small compared to the fractional changes in dimensions, thus suggesting that deformation takes place at approximately constant volume.

It is expected that the stress required for crack growth will increase with pressure because of the observed increase of the modulus. There may also be an increase in the effective surface energy because of the additional work that must be done against the confining forces to create new internal crack surface area. This will also cause an increase in the stress required for crack growth. Thus, pressure inhibits crack growth, and so the observed lack of surface cracking at elevated confining pressures and the shift to deformation by plastic flow are not unexpected. Therefore, there is a brittle-like to ductile transition as pressure is increased. Many brittle materials become ductile under hydrostatic pressure, and a similar transition has been observed in other materials [1,2,16].

The initial increase of the flow stress with increasing pressure at low pressures is, therefore, most probably due in part to an increase of the stress required for crack growth with increasing pressure. However, this increase may also be due in part to the transition of the failure mechanism from primarily crack processes to primarily plastic flow. The increase of the flow stress with increasing pressure may also be due to some of the same reasons as the increase in the modulus. The yield strength has been found to increase exponentially as porosity decreases in the same manner as the Young's modulus [30,33]. The flow stress considered here is expected to have

the same porosity dependence. In addition, the flow stress may increase with an increase in the glass transition temperature since the failure strength increases as temperature is decreased in the vicinity of the glass transition temperature at atmospheric pressure [15]. And finally, yield in the explosive or sucrose may become more significant as the yield strength of the binder increases as pressure is increased, thus accounting in part for the decreased sensitivity of the flow stress to pressure at higher pressures. Some of the yield relationships developed for polymers as a function of pressure may describe the pressure dependence of the flow stress observed in this work [20].

In summary, the same mechanisms that may determine the pressure dependence of the modulus may in part determine the pressure dependence of the flow stress. However, the pressure dependence of cracking appears to play a significant role in the pressure dependence of the flow stress at least at the lower pressures. Microscopic studies of deformed samples as a function of pressure during deformation should be helpful in determining the importance of crack processes.

General Pressure Dependence

As noted above, polymers exhibit the same general type of pressure dependence found here for the modulus and the flow stress (yield strength), that is, they both increase with pressure [20]. Thus, the results presented here support the conclusion made from the temperature and strain rate dependence of these same or similar quantities at atmospheric pressure, that is, that these mechanical properties are strongly influenced by the polymer content of these and similar composites [15]. This is true even though the polymer content of the composites being considered is a small percentage of the total (see Table 1).

Because the processes of plastic flow are not established at this time, it is not possible to ascribe a mechanism to the observed work hardening. The plastic flow and so the work hardening could take place primarily by dislocation

interactions in the particulate (sucrose or HMX) of the composite, or primarily by polymer processes in the binder. But whatever the mechanisms of plastic flow and work hardening, the efficiency of the work hardening process is increased by pressure. Additional studies are necessary to develop understanding of these processes.

As noted above, there are similarities in the stress-strain curves for PBS 9501, PBX 9501, and LX-14 that are not present in the curves for EDC37 [7] and PAX2A. The stress-strain curves for the former group of composites have linear regions that clearly define the modulus, the flow stress, and the work-hardening coefficient. The only common component of these composites is the polymer estane (see Table 1). Therefore, these common properties may be related to the properties of estane. Studies of estane alone may help to clarify this issue. The latter group of composites, EDC37 [7] and PAX2A, have stress-strain responses that curve continuously so that the modulus, the flow stress, and the work-hardening coefficient are not as well defined. This may be related to the presence of completely different binders and/or to the fact that they have larger concentrations of binder than PBS 9501, PBX 9501, and LX-14. Studies of the binder alone may also aid in the understanding of these properties.

Summary

The results indicate significant increases of the modulus, the flow stress, and the work-hardening coefficient with increasing pressure and the sensitivity of all three of these quantities to pressure decreases markedly with increasing pressure. The pressure dependence of the modulus is discussed in terms of several factors including the following: changes in porosity, a shift of the glass transition temperature, changes in the relative contributions of the binder and the explosive/sucrose to the modulus, and the effect of finite strains, all as a function of pressure. The pressure dependence of the flow stress may be due to some of these same factors, but is also influenced by the effect of pressure on crack growth processes.

Acknowledgments

The authors are indebted to D. Idar and B. Asay for providing the samples of PBS 9501 used in this work and to A. Lewis and C. Leppard for making the EDC37 samples available. This work was supported in part by AWE, Aldermaston, UK.

References

[1] Wiegand, D. A., J. Pinto, and N. Nicolaides. 1991. *J. Energetic Materials*, 9: 19–80.
[2] Pinto, J. and D. A. Wiegand. 1991. *J. Energetic Materials*, 9: 205–263.
[3] Mezgar, M., J. Pinto, and D. A. Wiegand. unpublished results.
[4] Structural Behavior Engineering Laboratory, Phoenix, Arizona.
[5] Wiegand, D. A. 2000. Technical Report ARWEC-TR-99009, U.S. Army Armament Research, Development and Engineering Center, Picatinny Arsenal, NJ.
[6] Pinto, J., S. Nicolaides, and D. A. Wiegand. 1985. Picatinny Arsenal Technical Report ARAED-TR-85004.
[7] Ellis, K., C. Leppard, B. Reddingius, and D. A. Wiegand. 2004. *35th Annual Conference of ICT, Energetic Materials, Structure and Properties, Karlsruhe, Federal Republic of Germany*, June.
[8] Harris, J. Private communication.
[9] Flowers, G. L. Private communication.
[10] Dobratz, B. M. and P. C. Crawford. 1985. *LLNL Explosive Handbook, Properties of Chemical Explosives and Explosive Simulants*, Lawrence Livermore National Laboratory Report UCRL-52997 Change 2, pp. 6–6 and pp. 8–6.
[11] Meakes, K. Private communication.
[12] Ellis, K. Private communication.
[13] Funk, D. J., G. W. Laabs, P. D. Peterson, and B. W. Asay. 1996. *Shock Compression of Condensed Matter 1995*, Woodbury, NY: pp. 145–148.
[14] Idar, D. Private communication.
[15] Wiegand, D. A. 1998. *Proceedings of the Eleventh International Detonation Symposium*, Snowmass, Colorado: p. 744.
[16] Wiegand, D. A. 2000. In M. D. Furnish, L. C. Chhabildas, and R. S. Hixon (eds.), *Shock Compression of Condensed Matter—1999*, New York: American Institute of Physics, p. 675.

[17] Wiegand, D. A. and B. Reddingius. 2003. In M. D. Furnish, Y. M. Gupta, and J. W. Forbes (eds.), *Shock Compression of Condensed Matter—2003*, New York: American Institute of Physics, p. 812.
[18] Lieb, R. J. 1996. Technical Report ARL-TR-1205, U.S. Army Research Laboratory, Aberdeen Proving Ground, MD, September.
[19] Wiegand, D. A. 2003. *Proceedings of the 12th International Detonation Symposium, San Diego, CA, August 2002*, in press, and *J. Energetic Materials*, 21: 125.
[20] Hoppel, C. P. R., T. A. Bogetti, and J. W. Gillespie, Jr. 1995. *J. Thermoplastic Composite Materials*, 8: 375.
[21] Constantino, M. and D. Ornellas. 1985. UCRL-92441.
[22] Constantino, M. and D. Ornellas. 1987. UCRL-95555.
[23] Ward, I. M. and D. W. Hardley. 1993. *An Introduction to the Mechanical Properties of Solid Polymers*, New York: John Wiley & Sons, pp. 234–236.
[24] Wiegand, D. A. unpublished results and to be published.
[25] Dienes, J. K. 1998. LA-UR-98–3620.
[26] Hodgman, C. D., ed. 1945. *Handbook of Chemistry and Physics*, 29th ed., Cleveland, Ohio: City Chemical Rubber Publishing Co.
[27] Boyer, H. E. and T. L. Gall, eds. 1985. *Handbook of Metals, Desk Edition*, Metals Park, Ohio: American Society for Metals.
[28] Trevino, S. F. and D. A. Wiegand. 1998. *Proceedings of the 21st Army Science Conference, Norfolk, VA, June*, p. 181.
[29] Wang, J. C. 1984. *J. Mat. Sci.*, 19: 801, 809.
[30] Wiegand, D. A. and J. Pinto. 1991. Picatinny Arsenal Technical Report ARAED-TR-91022.
[31] Patterson, M. S. 1964. *J. Appl. Phys.*, 35: 176.
[32] Wiegand, D. A. 1995/2003. *Proceedings of the 3rd International Conference on Deformation and Fracture of Composites, University of Surrey, Guildford, U.K.*, pp. 558–567, and *J. Energetic Materials*, 21: 109.
[33] Knudsen, F. P. 1959. *J. Am. Ceramic Soc.*, 42: 376.